Progress In Electromagnetics Research M, Vol. 107, 193–204, 2022

An Approximate Closed-Form Solution of Compensating for Beam Pointing Error with Uniform Linear Arrays

Shuaizhao Li[1, 2], Zhongjun Yu[1, 2, *], Qiang Zhang[1, 2], Chengxiang Hao[1, 2], and Ning Cui[1, 2]

Abstract—In phased array systems, beam pointing accuracy is one of the major issues for its great effect on radar communication. Regardless of the initial excitation error and the inherent mutual coupling between antenna elements, the anisotropy of antenna element's radiation pattern is the main reason for beam pointing error. In this paper, we propose a closed-form solution of compensating for beam pointing error with uniform linear arrays. It gives a theoretical explanation how beam pointing deviates from the desired angle when scanning angle and the number of elements vary. Then a numerical simulation validates the effectiveness of the proposed theory. Finally, an experiment with an X-band phased array verifies that the closed-form solution can be applied to practical phased array systems in the presence of mutual coupling.

1. INTRODUCTION

Phased arrays are widely utilized for military and civil use, including precise guidance and strike [1], the 5th Generation (5G) communication [2], automotive radar of unmanned vehicle [3], etc., which benefits from their abilities of beamforming, nulling, and beam steering. Accurate beam pointing is especially required for all these applications. However, there are three factors leading to beam pointing error.

The first is the amplitude and phase error between antenna elements. In practical phased array systems, the characteristic of components (including transmit/receive (T/R) module, power divider, etc.) might vary with each other, resulting in initial excitation amplitude and phase deviation. More uncertainty arises with temperature drift, device ageing, and the quantization error of phase shifts. Thus, phased array systems must get calibrated before operation. There has been great work to counter this problem, including rotating-element electric-field vector (REV) calibration method [4] and its improved versions [5–7], near-field measurement system-based method [8, 9], phase-toggling method [10, 11], and mutual coupling-based calibration [12, 13].

The second is the inherent mutual coupling between elements. Mutual coupling influences the performance of the antenna array by varying its element impedance, reflection coefficients, and overall antenna pattern, leading to beam pointing error. Many researches have been done to overcome this issue with algorithmic method [14] or by declining the coupling coefficients between antenna elements structurally, like electromagnetic bandgap (EBG) [15], defected ground structure (DGS) [16], the metamaterials [17], and decoupling network [18].

The last is the anisotropy of the radiation pattern of the antenna element. Even assuming that the two problems mentioned above do not exist, this factor still theoretically causes beam pointing deviation especially at a wide scan angle. To simplify the array synthesis issues, we tend to assume the radiation pattern of the antenna element to be isotropic. However, for practical scanning phased arrays,

Received 17 December 2021, Accepted 17 January 2022, Scheduled 21 January 2022
* Corresponding author: Zhongjun Yu (yuzj@ucas.ac.cn).
[1] Aerospace Information Research Institute, Chinese Academy of Sciences, Beijing 100190, China. [2] School of Electronic, Electrical and Communication Engineering, University of Chinese Academy of Sciences, Beijing 100190, China.

the maxima of the single element's radiated field and of the array factor are not both directed toward the desired scanning angle [19], causing beam pointing deviation. As far as we investigate, there have been few researches to figure out this problem. Phase synthesis for every channel utilizing optimization algorithm [20] can be a solution to obtain desired beam direction. However, it is impractical for beam control system because it consumes too much time and hardware resource. We give an approximate closed-form solution to compensate beam pointing error firstly with uniform linear arrays (ULAs). It is a simple but useful way to directly calculate the phase distribution of every channel. This on-line compensation solution can be applied to the practical beam control system normally with progressive phase distribution.

The outline of this paper is as follows. First, the analytical solution of compensating for beam pointing deviation with ULAs is derived in Section 2. In Section 3, to validate the compensation theory, a numerical simulation with a ULA without considering mutual coupling is carried out when beam pointing direction and the number of antenna elements are changed. Then in Section 4, to guarantee that the compensation theory is valid for practical phased array systems, experiments of an 11-element X-band ULA simulated with high-frequency structure simulator (HFSS) and measured in a microwave anechoic chamber are separately conducted. Finally, some conclusions are drawn in Section 5.

2. THEORY

Figure 1 shows the far-field geometry of a typical N-element ULA with spacing d, oriented in the direction θ. Assuming that all elements each with identical magnitude and a progressive phase β have identical far-field radiation pattern [19] in the absence of mutual coupling, the array factor can be derived as

$$AF(\theta) = \sum_{n=1}^{N} e^{j(n-1)(kd\sin\theta+\beta)} \tag{1}$$

where $k = 2\pi f/c_0$, $c_0 = 2.9979 \times 10^8$ m/s, and f is the operating frequency. To make the maximum radiation oriented in any direction θ_0 to form a scanning array, β should be adjusted so that

$$kd\sin\theta + \beta\,|_{\theta=\theta_0} = 0 \Rightarrow \beta = -kd\sin\theta_0 \tag{2}$$

Thus the array factor can be rewritten as

$$\begin{aligned} AF(\theta) &= \sum_{n=1}^{N} e^{j(n-1)kd(\sin\theta-\sin\theta_0)} \\ &= e^{j[(N-1)/2]kd(\sin\theta-\sin\theta_0)} \cdot \frac{\sin[Nkd(\sin\theta-\sin\theta_0)/2]}{\sin[kd(\sin\theta-\sin\theta_0)/2]} \end{aligned} \tag{3}$$

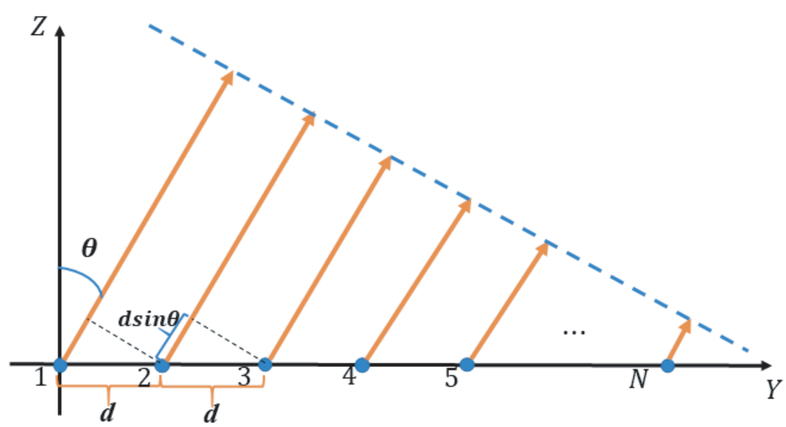

Figure 1. The far-field geometry of a typical N-element ULA.

If the reference point is the physical center of the array, the array factor is reduced to

$$AF(\theta) = \frac{\sin[Nkd(\sin\theta - \sin\theta_0)/2]}{\sin[kd(\sin\theta - \sin\theta_0)/2]} \tag{4}$$

Multiplied by the field $E(\theta)$ of a single element, the total field of the array is expressed by

$$\begin{aligned} T(\theta) &= E(\theta) \cdot AF(\theta) \\ &= E(\theta) \cdot \frac{\sin[Nkd(\sin\theta - \sin\theta_0)/2]}{\sin[kd(\sin\theta - \sin\theta_0)/2]} \end{aligned} \tag{5}$$

In most cases, $E(\theta)$ is not isotropic, leading to beam pointing deviation from the desired angle θ_0. Therefore, the progressive phase β must be adjusted as

$$\beta_x = -kd\sin\theta_x \tag{6}$$

where θ_x is called correction angle which should be at the neighborhood of θ_0. Then the total field of the array is rewritten as

$$T(\theta) = E(\theta) \cdot \frac{\sin[Nkd(\sin\theta - \sin\theta_x)/2]}{\sin[kd(\sin\theta - \sin\theta_x)/2]} \tag{7}$$

To make beam pointing precisely at θ_0, the condition that the derivative of $T(\theta)$ at θ_0 equals zero must be fulfilled.

$$\begin{aligned} \frac{dT(\theta)}{d\theta}\Big|_{\theta=\theta_0} &= -\frac{m\cos\theta_0 E(\theta_0)\cos(mb)\sin(Nmb)}{\sin^2(mb)} \\ &\quad + \frac{Nm\cos\theta_0 E(\theta_0)\cos(Nmb) + E'(\theta_0)\sin(Nmb)}{\sin(mb)} = 0 \end{aligned} \tag{8}$$

where $m = kd/2$, $b = \sin\theta_0 - \sin\theta_x$. It is reduced to

$$\tan(Nmb) = \frac{Nm\cos\theta_0 E(\theta_0)\tan(mb)}{m\cos\theta_0 E(\theta_0) - E'(\theta_0)\tan(mb)} \tag{9}$$

According to Taylor's theorem, when x tends to 0, $\tan x = x + x^3/3 + o(x^3)$. Thus the equation can be rewritten as

$$Nmb + \frac{(Nmb)^3}{3} = \frac{Nm\cos\theta_0 E(\theta_0)(mb + m^3b^3/3)}{m\cos\theta_0 E(\theta_0) - E'(\theta_0)(mb + m^3b^3/3)} \tag{10}$$

We simplify it as

$$b^2 - \frac{(N^2-1)\cos\theta_0 E(\theta_0)}{E'(\theta_0)} b + \frac{3}{m^2} = 0 \tag{11}$$

There are two possible solutions

$$b = \begin{cases} \dfrac{c + \sqrt{c^2 - \frac{12}{m^2}}}{2}, & \text{when } E'(\theta_0) \leq 0; \\ \dfrac{c - \sqrt{c^2 - \frac{12}{m^2}}}{2}, & \text{when } E'(\theta_0) > 0. \end{cases} \tag{12}$$

where $c = (N^2-1)\cos\theta_0 \frac{E(\theta_0)}{E'(\theta_0)}$. For the case $E'(\theta_0) \leq 0$

$$b = \sin\theta_0 - \sin\theta_x = \frac{c + \sqrt{c^2 - \frac{12}{m^2}}}{2} \tag{13}$$

According to $\sin\theta_0 - \sin\theta_x \approx \cos\theta_0(\theta_0 - \theta_x)$, we give an approximate solution of correction angle θ_x in Equation (14), which is a function of element number N, desired beam pointing angle θ_0, spacing d, operating frequency f, and far-field radiation pattern $E(\theta)$ of a single element.

$$\theta_x = \theta_0 - \frac{p + \sqrt{p^2 - \frac{12}{m^2\cos^2\theta_0}}}{2} \tag{14}$$

where $p=(N^2-1)\frac{E(\theta_0)}{E'(\theta_0)}<0$. Likewise for the case $E'(\theta_0)>0$

$$\theta_x=\theta_0-\frac{p-\sqrt{p^2-\frac{12}{m^2\cos^2\theta_0}}}{2} \tag{15}$$

From another perspective, θ_x is the angle which beam control system uses to calculate the phase distribution according to Equation (6). The actual beam direction is θ_0. The deviation between them, also called beam pointing error, can be obtained from Equation (16) for the case $E'(\theta_0)\le 0$.

$$\theta_x-\theta_0=-\frac{p+\sqrt{p^2-\frac{12}{m^2\cos^2\theta_0}}}{2} \tag{16}$$

It is easy to figure out the monotonicity of the function that the deviation between θ_x and θ_0 is bigger when the scanning angle θ_0 is wider, and the number N of the elements is smaller. It should be noted that the following equation has to be fulfilled to ensure the validity of the solution.

$$p^2-\frac{12}{m^2\cos^2\theta_0}\ge 0 \tag{17}$$

It is further reduced to

$$N\ge\sqrt{\frac{2\sqrt{3}}{m\cos\theta_0}\left|\frac{E'(\theta_0)}{E(\theta_0)}\right|+1} \tag{18}$$

However, it is hard to judge whether it is a big or small error simply according to the value of beam pointing error. A scientific method to evaluate the beam pointing error is to compare it with the half-power beamwidth (HPBW). Although $HPBW$ is theoretically affected by the anisotropy of the antenna element, the classical formula [21] listed as Equation (19) can be adopted as a reference.

$$HPBW=51\frac{\lambda}{Nd|\cos\theta_0|}(^\circ) \tag{19}$$

For practical phased systems in the presence of mutual coupling, if the array is large, most of the elements will see a uniform neighboring environment, and the active element pattern can be approximated as equal for all elements in the array [22]. Thus, the pattern of the full excited array can be expressed as the product of active element pattern and the array factor. The radiation pattern of the central element with all other elements terminated in matched loads is selected as $E(\theta)$. In addition, since $E(\theta)$ is obtained practically from the radiated field of discrete sampling angles, $E'(\theta_0)$ can be derived from the slope of the fitted curve of $E(\theta)$ or replaced with the following equation.

$$E'(\theta_0)\approx\frac{E(\theta_0+\Delta)-E(\theta_0-\Delta)}{2\Delta} \tag{20}$$

where Δ should be bigger than the beam pointing measurement accuracy in practical application.

For practical phased array systems, mainly four steps to compensate beam pointing error are summarized below.

(1) Obtain the active element pattern $E(\theta)$ of the ULA. This step can proceed in advance in an anechoic chamber. The radiation pattern of the central element with all other elements terminated in matched loads is measured, and the gain data at every angle are recorded.

(2) Extract the gain $E(\theta_0)$ and the slope of the gain $E'(\theta_0)$ of the active element pattern at the desired beam pointing angle θ_0.

(3) Calculate the correction angle θ_x by Equation (14) or (15) depending on the sign of $E'(\theta_0)$.

(4) Excite the array with progressive phase $\beta_x=-kd\sin\theta_x$ by beam control system.

3. NUMERICAL SIMULATION IN THE ABSENCE OF MUTUAL COUPLING

Assuming that there is a 12-element ULA with spacing $d=16$ mm operating at 9.5 GHz, and its radiated field $E(\theta)$ in YOZ plane of a single element equals $\cos\theta$. If the desired beam pointing direction θ_0 is 60° and $\beta=-kd\sin\theta_0$, the array's radiation pattern can be calculated by pattern multiplication using

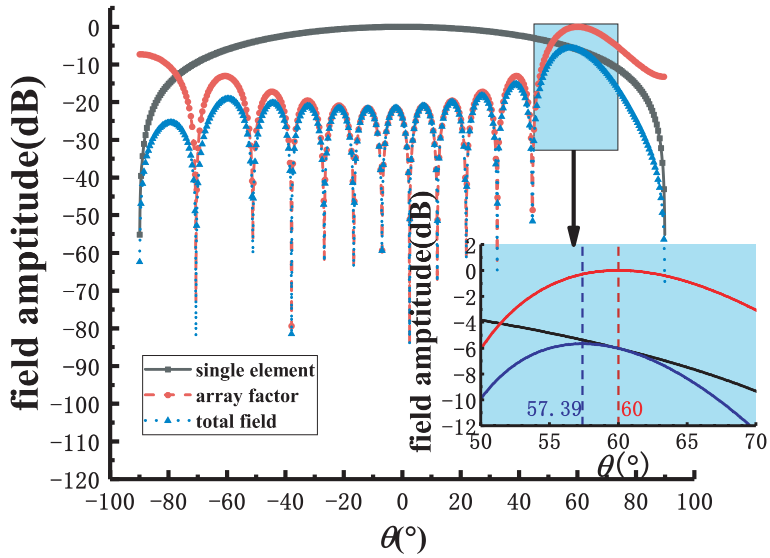

Figure 2. The radiation patterns of a single element, array factor and the whole array of a 12-element ULA with progressive phase $\beta = -kd\sin 60°$.

Equation (5) in the absence of mutual coupling. As a result of the anisotropy of antenna element's radiation pattern, the beam direction seen from Fig. 2 actually points at 57.39°, a non-negligible error compared to the desired angle.

Applied with the compensation theory using Equation (14), the correction angle $\theta_x = 63.29°$ is obtained. Replacing the progressive phase with $\beta = -kd\sin\theta_x$, the radiation pattern of the array is calculated with Equation (7), and its beam points at 59.92° seen from Fig. 3, quite close to the desired scanning angle. Likewise, the beam pointing results before compensation and after compensation are listed respectively as in Table 1 when the scanning angle varies and Table 2 when the number of antenna elements changes. As pointed out in Section 2, the deviation between θ_x and θ_0 is bigger when the scanning angle θ_0 is wider, and the number N of the elements is smaller. The beam pointing directions after compensation show good accordance with the desired angles. Thus, the correctness of the closed-form solution to compensate beam pointing error with ULAs gets validated.

Table 1. The beam pointing results of a 12-element ULA before compensation and after compensation when the scanning angle varies.

desired beam angle θ_0	10°	20°	30°	40°	50°	60°
beam pointing before compensation	9.91°	19.81°	29.64°	39.35°	48.75°	57.39°
correction angle θ_x	10.09°	20.2°	30.37°	40.68°	51.37°	63.29°
beam pointing after compensation	10°	20°	30°	40°	49.99°	59.92°

Table 2. The beam pointing results of a ULA with desired beam angle $\theta_0 = 60°$ before compensation and after compensation when the number of antenna elements changes.

the number N of elements	10	15	20	30	50	100
beam pointing before compensation	56.5°	58.21°	58.93°	59.5°	59.82°	59.95°
correction angle θ_x	64.75°	62.1°	61.18°	60.52°	60.19°	60.05°
beam pointing after compensation	59.84°	59.97°	59.99°	59.99°	60°	60°

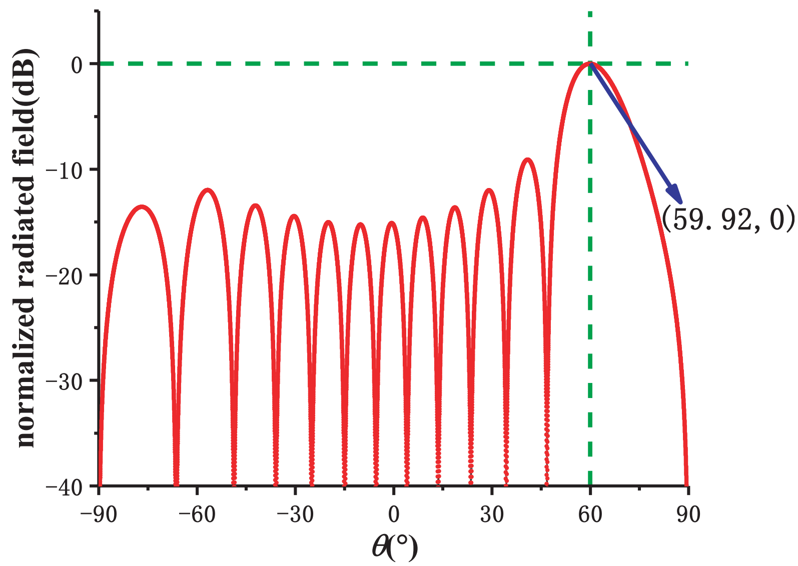

Figure 3. The radiation pattern of a 12-element ULA with progressive phase $\beta = -kd\sin 63.29°$.

4. EXPERIMENTS IN THE PRESENCE OF MUTUAL COUPLING

4.1. Simulation with HFSS

To validate the compensation theory in the presence of mutual coupling, an 11-element microstrip patch antenna array operating at 9.5 GHz is studied. The structures of the antenna element and its array are described by Fig. 4. The detailed parameters are described in Table 3, and the substrate material is Rogers 5880. The far-field radiation patterns of the element and the array in YOZ plane derived from electromagnetic simulator HFSS are shown as Fig. 5.

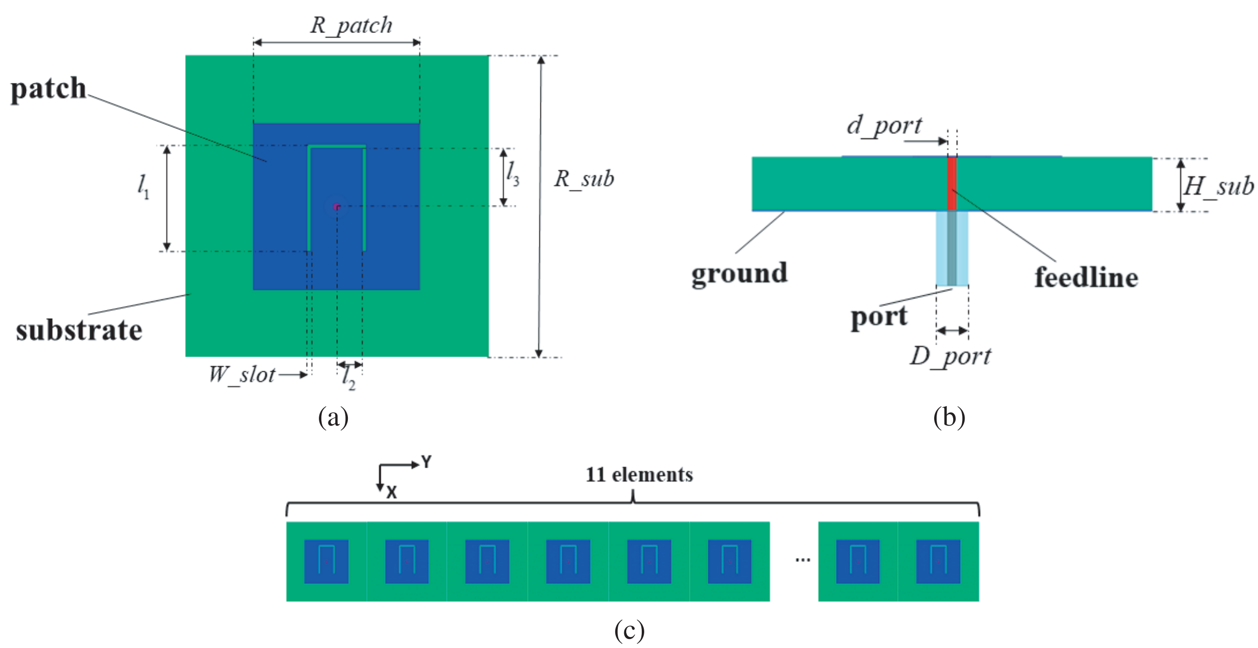

Figure 4. (a) Top view of the patch antenna. (b) Front view of the patch antenna. (c) The arrangement of the ULA.

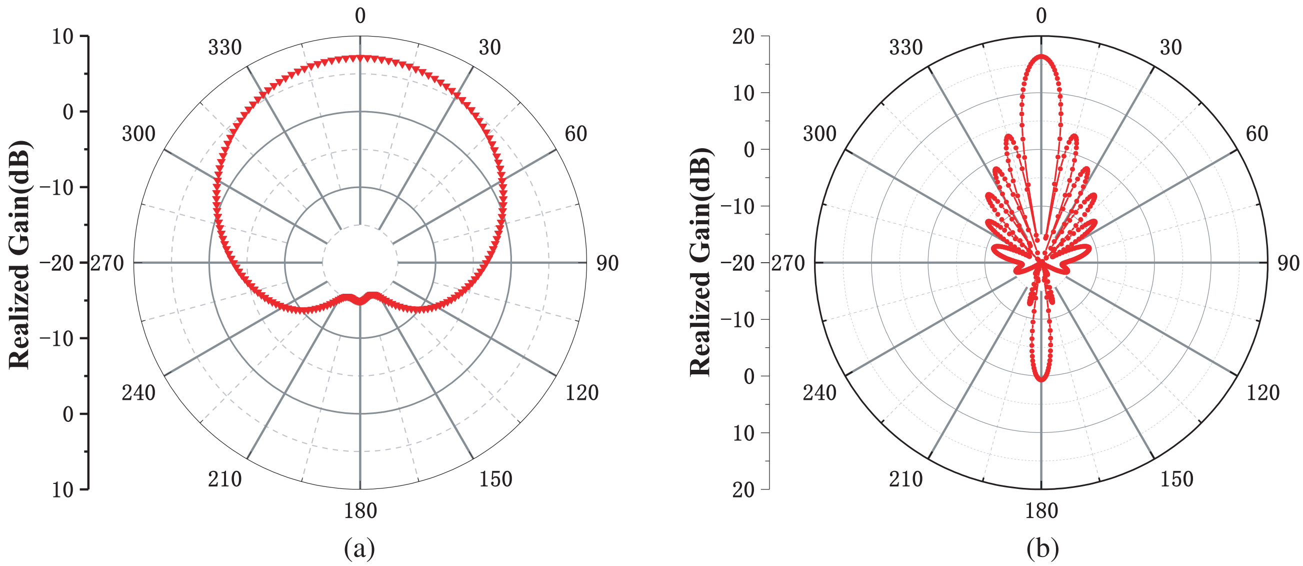

Figure 5. (a) The far-field radiation pattern in YOZ plane of a single element. (b) The far-field radiation pattern in YOZ plane of the array.

Table 3. The detailed parameters of the patch antenna.

antenna parameters	*R_sub*	*H_sub*	*R_patch*	*W_slot*	*l_1*	*l_2*	*l_3*	*D_port*	*d_port*
value(mm)	16	2.1	8.8	0.2	5.66	1.36	3.1	1.3	0.38

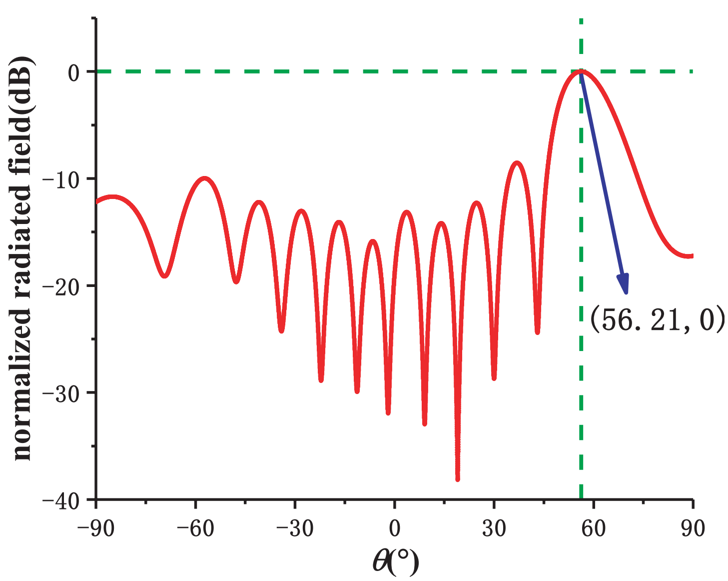

Figure 6. The simulated radiation pattern of an 11-element ULA with progressive phase $\beta = -kd\sin 60^\circ$.

Assuming that the desired steering angle $\theta_0 = 60^\circ$, and the array is excited by progressive phase $\beta = -kd\sin\theta_0$, the radiation pattern of the array in the presence of mutual coupling, as shown in Fig. 6, is simulated with HFSS. As seen from the result, the steering angle at the maximum gain declines to 56.21°, almost 4° error from the desired angle. To compensate the beam pointing error, firstly the active element pattern with a feed at the central element and with other elements terminated in matched loads is obtained by HFSS simulation, as shown in Fig. 7. Then, according to Equation (14), the correction angle $\theta_x = 64.9^\circ$ is derived. Replacing the excitation phase with progressive phase $\beta = -kd\sin\theta_x$, the radiation pattern of the fully excited array after compensation is simulated, as shown in Fig. 8. Results show that the beam points at 59.88°, quite close to the desired angle. Thus, the compensation theory can be applied to the situation in the presence of mutual coupling. The slight deviation from 60° is caused by the approximation of the compensation solution and the edge effect of the antenna array.

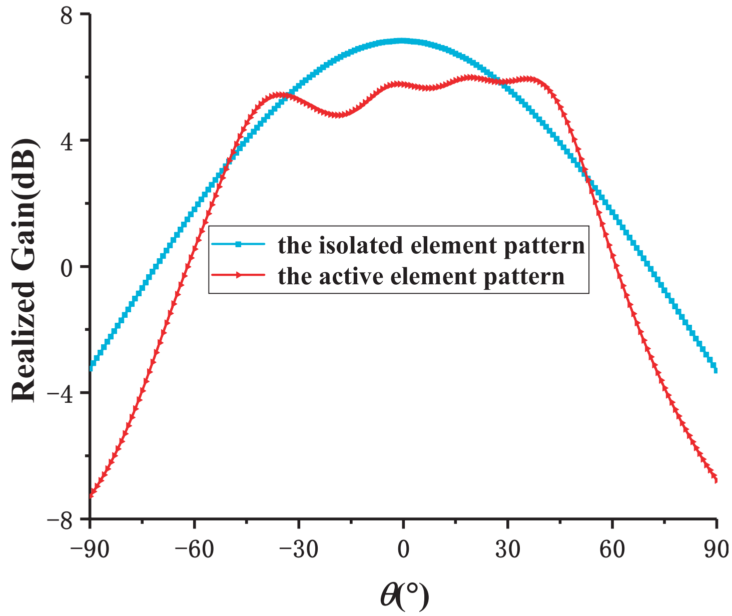

Figure 7. The simulated active element pattern.

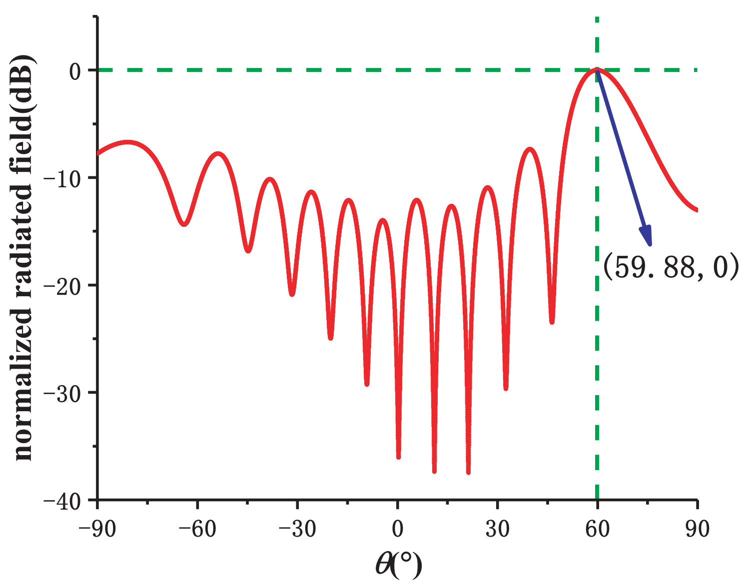

Figure 8. The simulated radiation pattern of an 11-element ULA after compensation with progressive phase $\beta = -kd\sin 64.9^\circ$.

4.2. Measurement in Anechoic Chamber

A two-dimension phased array operating at 9.5 GHz is available for our experiment with near field measurement system in an anechoic chamber, shown in Fig. 9. Since the compensation theory is only applied to ULA, an 11-element array is specially selected from the array as the experiment object, shown in Fig. 10. Only the radiation patterns in YOZ plane are considered.

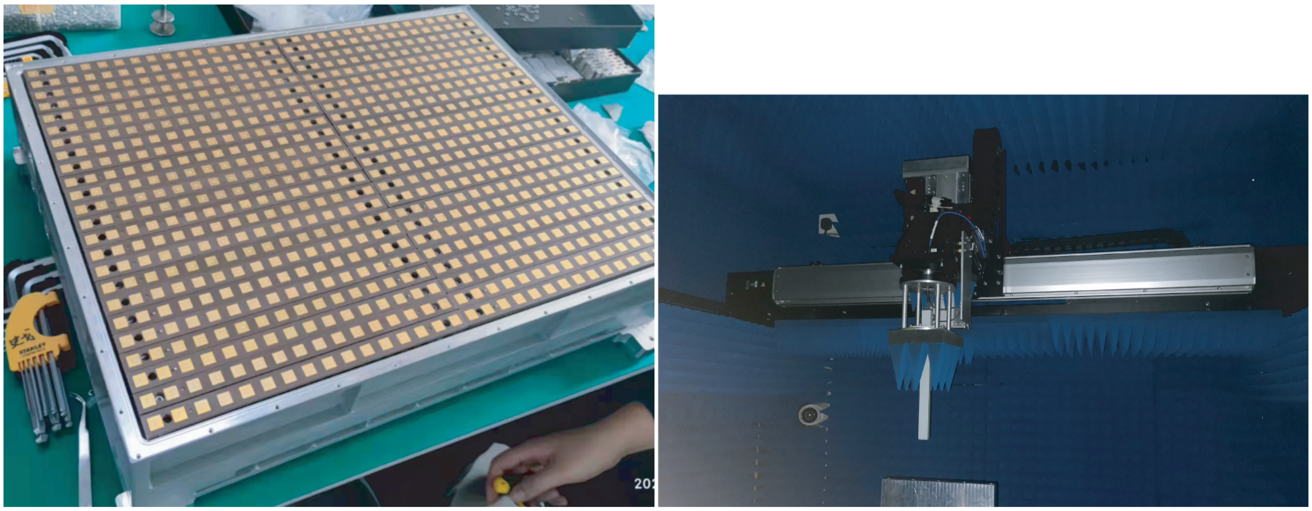

(a) (b)

Figure 9. (a) The two-dimension array available for experiment. (b) The near field measurement environment in anechoic chamber.

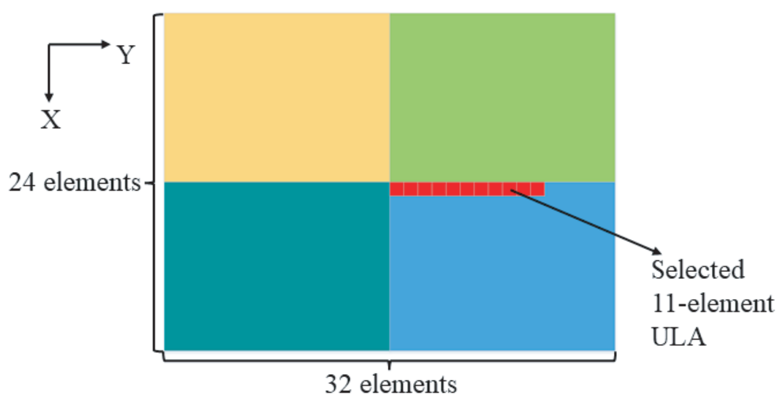

Figure 10. The arrangement of the array and the selected 11-element ULA for experiment.

Firstly, the active element pattern with a feed at the central antenna and with all other elements terminated in matched loads is measured and calculated by the near field measurement system, shown as Fig. 11.

Then in view of the situation that the array's beam scanning range is within $\pm 50°$. The desired beam direction is set at $\theta_0 = -45°$. Thus, the reference $HPBW$ can be calculated by Equation (19), which is 12.94°. The radiation pattern of the ULA excited by progressive phase $\beta = -kd\sin(-45°)$ is measured, shown in Fig. 12(a). As seen from the result, the actual beam direction is $-44.0°$, 7.73% of the $HPBW$ deviation from the desired angle.

Finally, according to the compensation theory using Equation (15) with the gain data and the slope of the gain at $-45°$ derived from the active element pattern, the correction angle θ_x calculated is $-46.3°$.

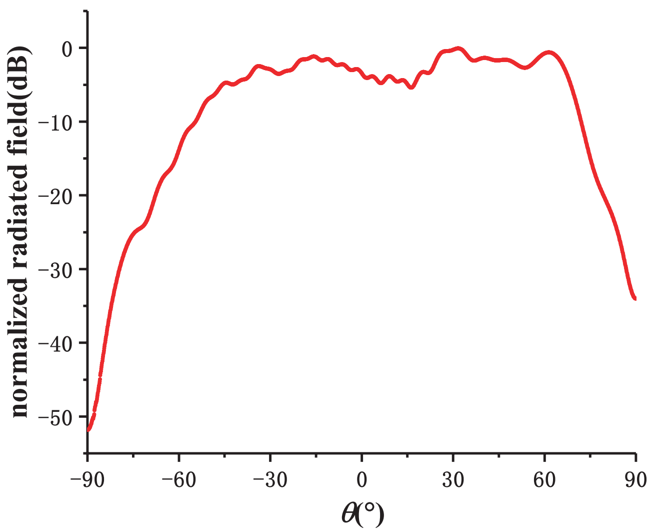

Figure 11. The measured active element pattern of the central element.

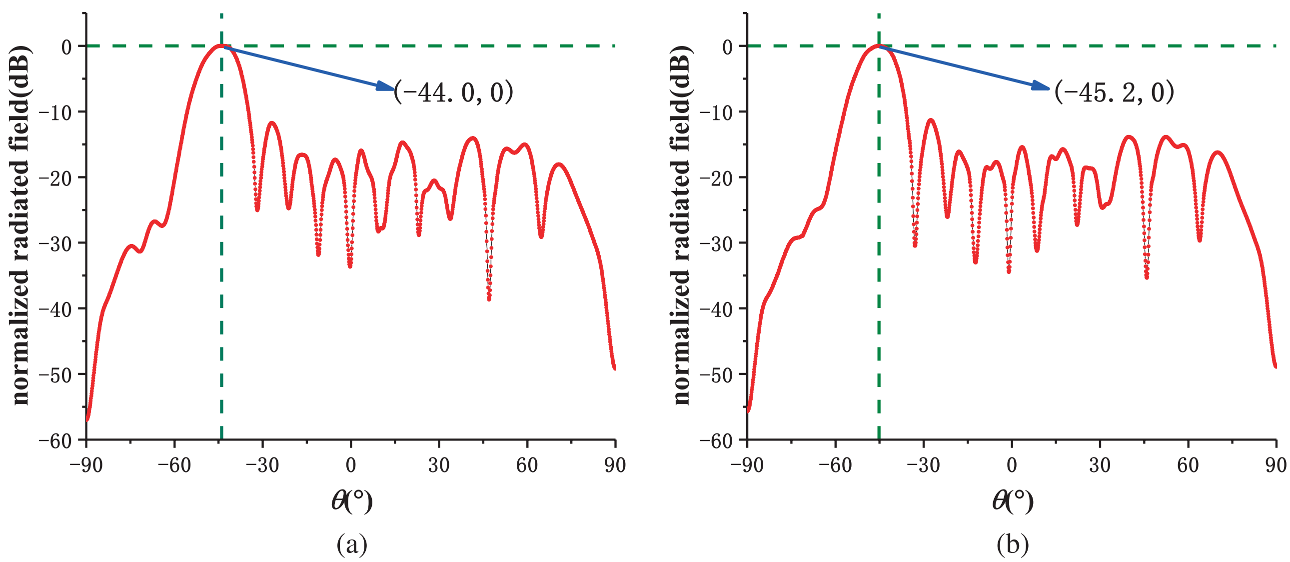

Figure 12. (a) The measured radiation pattern before compensation. (b) The measured radiation pattern after compensation.

Adjusting the array's excitation with progressive phase $\beta = -kd\sin(-46.3°)$, the radiation pattern after compensation is measured, shown as Fig. 12(b). The beam points at $-45.2°$, 1.55% of the $HPBW$ deviation from the desired angle. Although there is slight error, the values of the normalized gain at $-45°$ and $-45.2°$ are only 0.005 dB apart. Considering the issue of the beam pointing measurement accuracy, the compensation effect is acceptable.

5. CONCLUSION

In this paper, an approximate closed-form solution is proposed to compensate beam pointing error with ULAs mainly due to the anisotropy of antenna element's radiation pattern. It gives a theoretical explanation how beam pointing deviates from the desired angle when scanning angle and the number of elements vary. Numerical simulation and near field measurement experiment validate its effectiveness in both conditions: no mutual coupling and in the presence of mutual coupling. It is a simple and original way to directly give the phase distribution to compensate beam pointing error without complicated phase optimization, especially suited for practical beam control system offering progressive excitation phase. A solution of compensation for beam pointing error applied to two-dimension arrays is our next work.

REFERENCES

1. Rock, J. C., J. H. Mullins, J. P. Booth, and T. Hudson, "The past, present, and future of electronically-steerable phased arrays in defense applications," *2008 IEEE Aerospace Conference*, 1–7, 2008.
2. Flamini, R., C. Mazzucco, R. Lombardi, C. Massagrande, F. Morgia, and A. Milani, "Millimeter-wave phased arrays for 5G: An industry view on current issues and challenges," *2019 IEEE International Symposium on Phased Array System Technology (PAST)*, 1–2, 2019.
3. Soheil, Y., M.-A. Karim, and, M.-T. Mahmoud, "Low-cost comb-line-fed microstrip antenna arrays with low sidelobe level for 77 GHz automotive radar applications," *Progress In Electromagnetics Research M*, Vol. 94, 179–187, 2020.
4. Mano, S. and T. Katagi, "A method for measuring amplitude and phase of each radiating element of a phased array antenna," *Electronics and Communications in Japan (Part I: Communications)*, Vol. 65, No. 5, 58–64, 1982.
5. Sorace, R., "Phased array calibration," *IEEE Transactions on Antennas and Propagation*, Vol. 49, No. 4, 517–525, 2001.
6. Takahashi, T., Y. Konishi, and I. Chiba, "A novel amplitude-only measurement method to determine element fields in phased arrays," *IEEE Transactions on Antennas and Propagation*, Vol. 60, No. 7, 3222–3230, 2012.
7. Long, R., J. Ouyang, F. Yang, W. Han, and L. Zhou, "Fast amplitude-only measurement method for phased array calibration," *IEEE Transactions on Antennas and Propagation*, Vol. 65, No. 4, 1815–1822, 2017.
8. Long, R. and J. Ouyang, "Planar phased array calibration based on near-field measurement system," *Progress In Electromagnetics Research C*, Vol. 71, 23–31, 2017.
9. Lu, Y., L. Zhou, M. Cui, X. Du, and Y. Hu, "A method for planar phased array calibration," *Progress In Electromagnetics Research Letters*, Vol. 94, 19–25, 2020.
10. Lee, K.-M., Chu, R.-S., and S.-C. Liu, "A built-in performance-monitoring/fault isolation and correction (PM/FIC) system for active phased-array antennas," *IEEE Transactions on Antennas and Propagation*, Vol. 41, No. 11, 1530–1540, 1993.
11. Long, R., J. Ouyang, F. Yang, W. Han, and L. Zhou, "Multi-element phased array calibration method by solving linear equations," *IEEE Transactions on Antennas and Propagation*, Vol. 65, No. 6, 2931–2939, 2017.
12. Aumann, H. M., A. J. Fenn, and F. G. Willwerth, "Phased array antenna calibration and pattern prediction using mutual coupling measurements," *IEEE Transactions on Antennas and Propagation*, Vol. 37, No. 7, 844–850, 1989.
13. Nafe, A., K. Kibaroglu, M. Sayginer, and G. M. Rebeiz, "An in-situ self-test and self-calibration technique utilizing antenna mutual coupling for 5G multi-beam TRX phased arrays," *2019 IEEE MTT-S International Microwave Symposium (IMS)*, 1229–1232, 2019.
14. Bao, J., Q. Huang, X. H. Wang, P. Liu, and X.-W. Shi, "Mutual coupling calibration for L-shaped microstrip antenna array with accurate 2-D direction of arrival estimation," *Progress In Electromagnetics Research Letters*, Vol. 57, 9–16, 2015.
15. Fang, Y. and Y. Rahmat-Samii, "Microstrip antennas integrated with Electromagnetic Band-Gap (EBG) structures: A low mutual coupling design for array applications," *IEEE Transactions on Antennas and Propagation*, Vol. 51, No. 10, 2936–2946, 2003.
16. Chiu, C.-Y., C.-H. Cheng, R. D. Murch, and C. R. Rowell, "Reduction of mutual coupling between closely-packed antenna elements," *IEEE Transactions on Antennas and Propagation*, Vol. 55, No. 6, 1732–1738, 2007.

17. Yang, X. M., X. G. Liu, X. Y. Zhou, and T. J. Cui, "Reduction of mutual coupling between closely packed patch antennas using waveguided metamaterials," *IEEE Antennas and Wireless Propagation Letters*, Vol. 11, 389–391, 2012.
18. Xia, R.-L., S.-W. Qu, P.-F. Li, D. Q. Yang, S. Yang, and Z.-P. Nie, "Wide-angle scanning phased array using an efficient decoupling network," *IEEE Transactions on Antennas and Propagation*, Vol. 63, No. 11, 5161–5165, 2015.
19. Balanis, C. A., *Antenna Theory: Analysis and Design*, Wiley, Hoboken, 2016.
20. Malek, N. A., K. K. Anuar, O. O. Khalifa, and M. R. Islam, "Comparison of unit-cell and all-cells active element patterns of small antenna array," *2020 IEEE International RF and Microwave Conference (RFM)*, 1–4, 2020.
21. Mailloux, R. J., *Phased Array Antenna Handbook*, Artech House, Norwood, 2017.
22. Pozar, D. M., "The active element pattern," *IEEE Transactions on Antennas and Propagation*, Vol. 42, No. 8, 1176–1178, 1994.